Research Article

Shengwen Yin*, Yawen Lu, and Yu Bai

Interval models for uncertainty analysis and degradation prediction of the mechanical properties of rubber

https://doi.org/10.1515/rams-2023-0142
received June 13, 2023; accepted October 13, 2023

Abstract: As rubber is a hyperelastic material, its nonlinear deformation behavior during aging is significantly influenced by various factors, including the material characteristics, demonstrating a significant uncertainty. Most of the existing uncertain prediction methods of rubber nonlinear property degradation are based on the probability density function, which requires a large number of samples to obtain the probability distribution and requires a lot of work. Therefore, the interval model is used in this study to characterize the uncertainty. However, the traditional interval constitutive models ignore the correlation between interval variables, and the prediction results have large errors. In order to minimize prediction errors and improve prediction accuracy, an interval Mooney–Rivlin (M–R) correlation model that considers the correlation between parameters was established. To address the influence of uncertainties, an interval Arrhenius model was constructed. The M–R model requires multiple fittings of stress–strain curves to obtain the model parameters, and the prediction process is relatively complex. Therefore, combing the two proposed models, the relationship equations of rubber tensile stress with aging temperature and aging time were first established by interval Arrhenius, and then the interval M–R model was used to obtain the variation ranges of parameters C_{10} and C_{01}. By contrasting this with the measured rubber aging information, the effectiveness of the proposed model was confirmed. Compared with the prediction model based on the average value, the maximum error of prediction of this model is reduced by about 60%. Compared with the traditional interval model, the prediction region is significantly reduced, which further improves the prediction accuracy. The above results indicate that this interval aging lifetime prediction model is suitable for characterizing the nonlinear stress–strain behavior of rubber-like elastomers.

Keywords: rubber aging prediction method, interval Mooney–Rivlin correlation model, thermally accelerated aging test, uncertainty

1 Introduction

Rubber materials are widely used in major fields, such as vibration isolation, damping, and energy absorption, owing to their high wear resistance, tear resistance, deformation recoverability, and compression elongation [1]. During long-term use, rubber is affected by temperature, oxidation, stress, as well as the degradation of its mechanical properties, which is known as the aging phenomenon. This aging process affects not only the material performance but also its service life. Therefore, there is a high theoretical relevance and practical engineering benefit in studying the prediction of mechanical quality degradation [2,3].

Long-term thermo-oxidative degradation of any polymer is a problem under normal environmental conditions unless a sealed system is used or inert conditions are deliberately introduced. Therefore, thermally driven degradation is a focal point in the field of “polymer degradation and stability” [4]. In thermo-oxidative aging studies of rubber materials, the accelerated aging test is widely used as an effective method to obtain performance index data [5,6]. The Arrhenius model is favored by researchers in accelerated lifetime tests [7–11] and is widely used for life prediction of polymers in different environments (especially temperature) [12,13]. The reason for this common application is that the method is easy to implement and is relevant in some cases [14]. However, as research has progressed, more results have shown the limitations of the Arrhenius model [15–17]. To cope with different

* **Corresponding author: Shengwen Yin,** Key Laboratory of Traffic Safety on Track, Ministry of Education, School of Traffic & Transportation Engineering, Central South University, Changsha 410000, China, e-mail: shengwen@csu.edu.cn
Yawen Lu, Yu Bai: Key Laboratory of Traffic Safety on Track, Ministry of Education, School of Traffic & Transportation Engineering, Central South University, Changsha 410000, China

aging conditions, some scholars conducted a series of studies using the traditional Arrhenius model, and various improved Arrhenius-modified models were successively proposed [18–24].

Moreover, because rubber is a hyperelastic material, its deformation in actual engineering exhibits strong nonlinear features, and a suitable nonlinear model must be chosen to characterize the material stress–strain properties [25,26]. In the field of hyperelastic modeling, Khaniki *et al.* [27] discussed the traditional hyperelastic strain energy density models such as neo-Hookean, Mooney–Rivlin (M–R), Ogden, Polynomial, Arruda–Boyce, Yeoh, and Gent. These intrinsic models are now present in many studies and used to understand the nonlinear mechanical behavior of different structures (hyperelastic shells, hyperelastic plates, hyperelastic beams, *etc.*) [28–30]. For rubber-like materials, Destrade *et al.* [31] pointed out that the core of the modeling problem is not related to the functional form of the strain energy, but depends on the method of fitting and the way of reading the data. Whereas before, Marckmann and Verron [32] had already pointed out in their study the applicability of the M–R model for describing the nonlinear mechanical properties of rubber-like materials at small and medium strains (less than 200%). And the study by Puglisi and Saccomandi [33] points out that while Mooney's theory does not provide a satisfactory and self-consistent basis for the properties of rubber in the most general strain states, a comparison of its predictions with experimental data suggests that the model is more predictive than the neo-Hookean model. As research progresses, more and more hyperelastic constitutive models have been proposed that begin to take into account environmental aging factors such as temperature, time, and humidity [34,35].

However, in an actual service process, the degradation of the mechanical properties of rubber products presents many uncertainties, and this affects the deformation behavior of the mechanical components, such as rubber sealing components [36]. If the aforementioned deterministic model is used for prediction, the results contain large errors. To address these problems, Liu *et al.* [37] combined Monte Carlo and Bayesian averaging methods to establish new aging prediction models. Varga *et al.* [38] proposed a model based on a two-dimensional normal probability density function (PDF) algorithm to generate the transformed Arrhenius parameter InA and E/R histogram. Woo *et al.* [39] and Shao and Kang [40] predicted the longevity of a sealed structure using the finite element approach and physics of the failure method, respectively. Korba *et al.* [41] proposed a hyperelastic intrinsic model for a weight function based (WFB) model that considers the effects of aging temperature and duration.

All the above methods have certain shortcomings: the method that introduces Bayes can only guarantee accuracy at the p-quantile, the algorithm of László Varga *et al.* requires solving probability distributions, the method of Woo and Shao considers only the random distribution of one parameter, and the WFB principal structure model requires a long experimental testing time. In summary, the existing literature analyzes the uncertainty from the stochastic, statistical top and requires obtaining the probability distribution function before predicting the performance degradation of a rubber material. The prerequisite for the use of these methods is sufficient statistical information; otherwise, it is difficult to determine the probability density function of the parameter. For small sample data, the interval model method with nonprobability statistics is more appropriate [42,43]. However, the traditional interval method typically directly introduces multiple interval variables, and the influence of aging conditions on interval model parameters and the constraint relationship between variables are often ignored. This can lead to inaccuracies between the predicted range of interval variables and the actual, generating large prediction errors and increasing the complexity of uncertainty estimation.

To further reduce the workload of existing uncertainty prediction methods and simplify the prediction process while improving the prediction accuracy, this study proposes an interval acceleration prediction method based on the Arrhenius and M–R models, which includes the interval Arrhenius and interval M–R correlation models. The interval Arrhenius model converts the interval uncertainty problem into a deterministic problem, and the latter is used to accurately describe the nonlinear characteristics of rubber materials during deformation. Based on the performance degradation data of rubber, the interval Arrhenius model was constructed by considering the tensile stress of rubber at different strain rates as the performance degradation index, and the interval correlation model, which can accurately characterize material stress–strain properties, was established by considering the parameter correlation. To confirm the accuracy of the proposed model, thermally accelerated aging tests were conducted on rubber at predetermined temperatures. The results showed that the prediction intervals obtained using this method accurately correlate with the actual values. Therefore, the method proposed in this work can effectively avoid the influence of interval expansion on the accuracy of prediction results and achieve accurate prediction of service rubber performance degradation, which is of great benefit for the improvement of material performance and quality as well as the lifetime evaluation of rubber sealing material products made from the production process, and this is also of great significance for the stable development of China's industrial field.

2 Materials and tests

2.1 Materials

In this study, rectangular chloroprene rubber plates were used as the test material. All the rubber samples were 150 × 130 × 2 mm in size, which were produced especially for this experiment. Figure 1 shows the rubber sheets used in the test. The main mechanical properties and composition of the material are shown in Tables 1 and 2, respectively.

Table 2: Material recipes

Ingredient	Proportion
Chloroprene rubber	100
Carbon black	30
Magnesium oxide	4
Zinc oxide	5
Stearic acid	1.5
Accelerator	2.5
P-phenylenediamine antioxidant	2
Diphenylamine antioxidant	2

2.2 Accelerated aging test for rubber

The rubber thermal oxidation aging test was conducted based on the ISO188 standard. The number of samples was adjusted to ten to account for the possible dispersion of mechanical behavior among the various rubber specimens. To ensure the efficiency of the accelerated test and avoid the influence of excessive accelerated aging temperature on the aging mechanism of rubber, the temperatures were set to 70, 80, 90, and 100°C. The specimens were placed in an air-circulating oven during the experiments, as shown in Figure 2. Since the degradation of rubber properties with aging often follows an exponential function, the time points for testing the mechanical properties of materials are usually set dense initially and then sparse. For every 10°C increase in temperature, the aging rate increases by a factor of roughly 0.5–1, so the total aging time setting becomes progressively less as the aging temperature increases. Table 3 lists the time-points set for the mechanical properties of the rubber tested in this study.

When the set aging time was reached, the rubber samples were removed from the oven and then cooled at room temperature for more than 24 h.

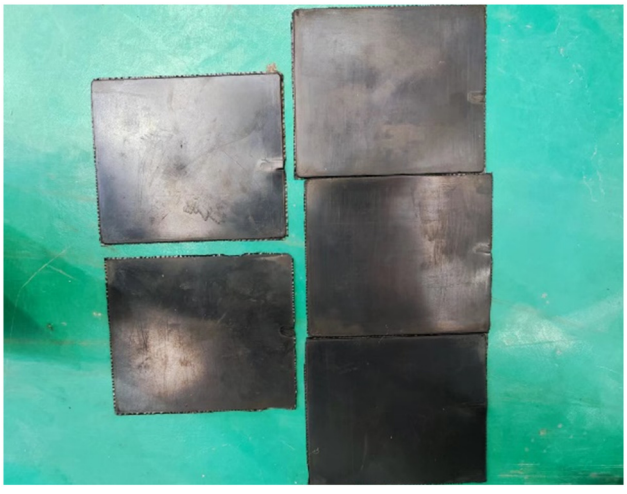

Figure 1: Specific dimensions of the tested rubber sheets.

Table 1: Main mechanical properties of unaged rubber

Mechanical properties	Values
Shore hardness (ha)	52
Density (g·cm^{-3})	1.25
Tensile strength (MPa)	16.2
Ductility (%)	657

2.3 Tensile test

To obtain uniaxial tensile specimens of the rubber materials, we cut the aged rubber pieces into dumbbell-shaped specimens using a cutter, as shown in Figure 3. The

Figure 2: High-temperature test oven for rubber aging.

Table 3: High-temperature airbag rubber performance aging test time-points

	Test temperature (°C)			
	70	**80**	**90**	**100**
Test time node (days)	0	0	0	0
	2	1	1	0.5
	4	2	2	1
	8	4	4	2
	16	8	7	4
	24	16	14	8

Figure 3: Tensile specimen.

dumbbell-shaped specimens used in this study were 45 mm long, 6 mm wide, and 2 mm thick. At the laboratory temperature (23 ± 2°C), the uniaxial tensile test was conducted on the aged rubber plates according to ASTM D412 to obtain the change rule of the mechanical performance of aging rubber.

The tensile tests were performed on a universal testing machine, equipped with a 5 kN load cell. During the experiment, the dumbbell-shaped specimens were vertically clamped between two fixtures with 10 ± 0.5 mm at the top and bottom, so that the tensile force was evenly loaded onto the cross-section. The tensile fixture controls the elongation of the rubber samples through a fixed limiter, and in this study, the maximum displacement is set to 20 mm, which enables the maximum strain of the rubber specimens to reach 80% in all cases. Five cyclic tensile testing (rate: 50 mm·min^{-1}) were conducted on the cut specimens at each test node. Figure 4 shows the cyclic tensile results of a rubber specimen after the test. As shown in the figure, the rubber exhibits a stress-softening phenomenon. After each stretch, the deformation force required for the same strain in the rubber decreases. The force–displacement curve remains the same after five cycles. This phenomenon is known as the Mullins effect, also referred to as stress softening. To eliminate this effect and obtain more accurate data, we conducted five cyclic tensile tests on each sample and then took the result of the sixth tensile test after the cycle as the final test data. For each aging condition, ten samples were tested and the results were averaged. Figure 5 shows the average stress–strain curves for 4 days of aging at different temperatures.

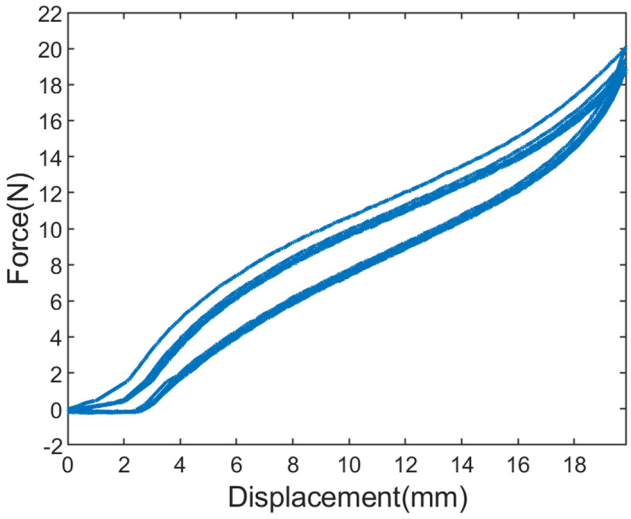

Figure 4: Cyclic tensile results of a rubber specimen.

It is evident from the preliminary examination of the data in Figure 5 that the rubber experiences an increase in tensile stress with temperature over the course of the same aging process. Rubber aging is accelerated by temperature, and high temperatures cause it to proceed quickly. The stress–strain curves of different rubber samples at the same aging time at a fixed temperature are obviously different, showing a large dispersion. The dispersion of the properties of the rubber samples increase as the strain rate increases, indicating that the uncertainty of the rubber material is variable.

The range of rubber tensile stresses with respect to time at the set temperature was obtained based on the

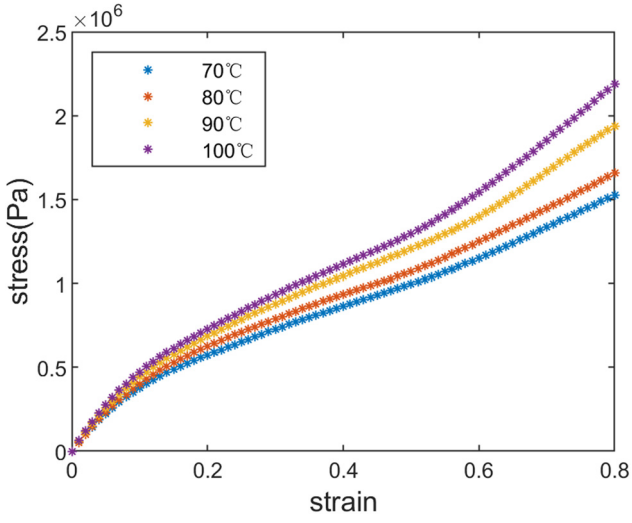

Figure 5: The average stress–strain curves for 4 days of aging at different temperatures.

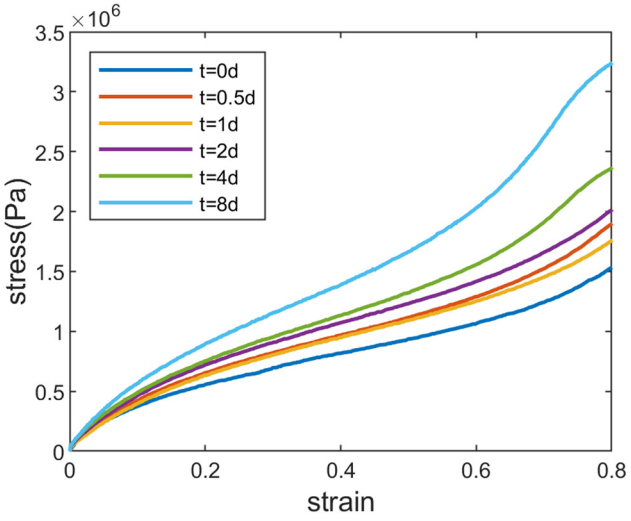

Figure 6: Average stress–strain curves for ten specimens at 100°C.

stress–strain curves obtained at each test node. Figure 6 shows the average stress–strain curves of the specimens at 100°C with aging time. Figure 6 shows that the stress at the same strain rate varies with aging time; therefore, the tensile stress at each strain rate can be used as the performance degradation index parameter of the rubber material. The stress–strain curves from the test were processed, and the ratio of maximum stress to minimum stress at each strain rate was obtained by selecting 30, 60 and 90% strain rates. Table 4 shows the ratio of maximum stress to minimum stress for several samples at three strain rates at 100°C. Table 4 also shows that the stress fluctuations of the rubber at the same strain rate increase with aging time, indicating that the uncertainty of the material is variable.

Table 4: Ratio of the maximum stress to the minimum stress for a specimen under three strain rates at 100°C

Aging time (days)	Strain		
	0.3	0.6	0.9
0.5	1.0896	1.1147	1.1165
1	1.1005	1.1200	1.1276
2	1.1123	1.1306	1.1389
4	1.1167	1.1542	1.1887
8	1.1360	1.1832	1.3216

3 Date processing in the accelerated test

3.1 Interval acceleration prediction model

During the service of air springs, external forces on the rubber material are uncertain, and their deformation exhibits strong nonlinear characteristics. To effectively simulate the mechanical behavior of rubber materials, a suitable nonlinear model must be used to describe their stress–strain characteristics. When temperature is utilized as the accelerating stress, the Arrhenius model is typically employed as an acceleration model. In this study, the interval Arrhenius and M–R models were introduced to establish an interval acceleration prediction model that considers the influence of the uncertainty and correlation between parameters. To simplify the prediction process, an interval model of rubber tensile stress at different strain rates was directly established and converted into interval expressions of C_{10} and C_{01} based on the interval M–R correlation model.

3.1.1 Interval M–R correlation model

At present, many types of intrinsic hyperelastic models exist for rubber materials, and for the stress–strain characteristics of rubber materials, the M–R model parameters are usually used to describe them. The M–R model, which is widely used in engineering, is expressed as follows:

$$W = \sum_{r=0}^{\infty}\sum_{s=0}^{\infty} C_{rs}(I_1 - 3)^r(I_2 - 3)^s, \tag{1}$$

where W is the strain–energy function per unit of undeformed volume, C_{rs} is the material parameter, and I_1 and I_2 are the first and second strain variables. Eq. (1) takes the following form if the M–R model with two parameters is applied:

$$W = C_{10}(I_1 - 3) + C_{01}(I_2 - 3). \tag{2}$$

Assuming that the material is incompressible, the stress–strain relationship for the M–R constitutive model can be derived for the special case of uniaxial tension as follows:

$$\frac{\sigma}{2(\lambda - \lambda^{-2})} = C_{10} + \frac{C_{01}}{\lambda}, \tag{3}$$

where σ denotes the engineering stress value at the tensile ratio. Letting $Y = \frac{\sigma}{2(\lambda - \lambda^{-2})}$, $X = 1/\lambda$, $a_1 = C_{01}$, and $b_1 = C_{10}$, Eq. (3) can be changed to the following equation:

$$Y_1 = b_1 + a_1 X_1. \tag{4}$$

The interval M–R model proposed in this study introduces interval variables a_1^I and b_1^I based on the traditional model. Then, Eq. (4) can be written as follows:

$$Y_1 = b_1^I + a_1^I X_1, \tag{5}$$

where $a_1^I = C_{01}^I$ and $b_1^I = C_{10}^I$. Owing to the change in the interval parameters, the Eq. (5) has three cases, as shown in Eq. (6). Four schematic lines are introduced, denoted as $Y_i (i = 1, 2, 3, 4)$, and the corresponding parameters are $a_i (i = 1, 2, 3, 4)$ and $b_i (i = 1, 2, 3, 4)$. Figure 7 shows a schematic of the interval correlation model.

$$b^I \in \begin{cases} [b_1, b_3], \text{if } a^I \in [a_3, a_1] \\ [b_1, b_2], \text{if } a^I \in [a_1, a_2] \\ [b_4, b_2], \text{if } a^I \in [a_2, a_4] \end{cases}. \tag{6}$$

The blue and pink areas in Figure 7 are the interval expansions, which are caused by ignoring the correlation between the two parameters a^I and b^I. When the value of a^I is the maximum value a_4, if parameter b^I is arbitrarily valued in the range of $[b_4, b_3]$, it will lead to an expansion of the upper interval. When the value of a^I is the minimum value a_3, if parameter b^I is arbitrarily valued in the range of $[b_4, b_3]$, it will lead to an expansion of the upper interval.

Therefore, when the slope parameter a^I of the linear equation varies within the range of $[\underline{a}, \bar{a}]$, the fitted line is ensured to be within the fitted area to minimize the interval expansion. In other words, the fitted interval curve must satisfy Eq. (7) for X_1 and X_m.

$$\begin{cases} Y(X_1) \geq \min\{Y_1(X_1), Y_4(X_1)\}, \\ Y(X_1) \leq \max\{Y_2(X_1), Y_3(X_1)\}, \\ Y(X_m) \geq \min\{Y_1(X_m), Y_3(X_m)\}, \\ Y(X_m) \leq \max\{Y_2(X_m), Y_4(X_m)\}. \end{cases} \tag{7}$$

Here $X_1 \in [0, X_m)$. Combined with Eq. (5), the relationship between interval variables a^I and b^I is shown in Eq. (8).

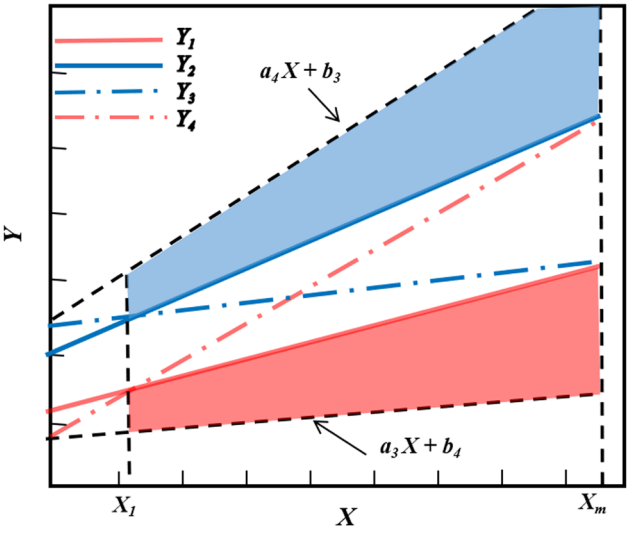

Figure 7: Schematic of the interval correlation model.

$$\begin{cases} b^I \geq \min\{Y_1(X_1), Y_4(X_1)\} - a^I X_1, \\ b^I \leq \max\{Y_2(X_1), Y_3(X_1)\} - a^I X_1, \\ b^I \geq \min\{Y_2(X_m), Y_4(X_m)\} - a^I X_m, \\ b^I \leq \max\{Y_1(X_m), Y_3(X_m)\} - a^I X_m. \end{cases} \tag{8}$$

The three cases in Eq. (6) are analyzed. During $a^I \in [a_3, a_1]$, the lower boundary of the fitted curve is the lower boundary of the fitted region, and only the fitted line of the upper boundary must satisfy the X_1 and X_m values in the fitted region. During $a^I \in [a_1, a_2]$, the upper and lower boundaries of the fitted curve are the boundaries of the fitted region, and the relationship between the parameters is given by Eq. (9). During $a^I \in [a_2, a_4]$, the upper boundary of the fitted curve is the upper boundary of the fitted region, and only the fitted line at the lower boundary must satisfy the X_1 and X_m values within the fitted region. Therefore, Eq. (8) can be written as follows:

$$b^I \in \begin{cases} [\min\{Y_1(X_m), Y_3(X_m)\} - a^I X_m, \ \max\{Y_2(X_1), Y_3(X_1)\} \\ \quad - a^I X_1], \text{for } a^I \in [a_3, a_1] \\ [\min\{Y_1(X_1), Y_4(X_1)\} - a^I X_1, \ \max\{Y_2(X_1), Y_3(X_1)\} \\ \quad - a^I X_1], \text{for } a^I \in [a_1, a_2] \\ [\min\{Y_1(X_1), Y_4(X_1)\} - a^I X_1, \ \max\{Y_2(X_m), Y_4(X_m)\} \\ \quad - a^I X_m], \text{for } a^I \in [a_2, a_4] \end{cases}. \tag{9}$$

Eq. (10) represents the rewritten Eq. (5). Given $a_1^I = C_{01}^I$ and $b_1^I = C_{10}^I$, the relevant model of the parameters is shown in Eq. (11).

$$\frac{\sigma}{2(\lambda - \lambda^{-2})} = C_{10}{}^I + \frac{C_{01}{}^I}{\lambda}, \tag{10}$$

$$\begin{cases} C_{10}^I \geq \min\{Y_1(1/\lambda_m), Y_3(1/\lambda_m)\} - C_{01}^I/\lambda_m \\ C_{10}^I \leq \max\{Y_2(1/\lambda_1), Y_3(1/\lambda_1)\} - C_{01}^I/\lambda_1 \\ \quad \in [a_3, a_1], \end{cases} \text{for } C_{01}^I$$
$$\begin{cases} C_{10}^I \geq \min\{Y_1(1/\lambda_1), Y_4(1/\lambda_1)\} - C_{01}^I/\lambda_1 \\ C_{10}^I \leq \max\{Y_2(1/\lambda_1), Y_3(1/\lambda_1)\} - C_{01}^I/\lambda_1 \\ \quad \in [a_1, a_2], \end{cases} \text{for } C_{01}^I \tag{11}$$
$$\begin{cases} C_{10}^I \geq \min\{Y_1(1/\lambda_1), Y_4(1/\lambda_1)\} - C_{01}^I/\lambda_1 \\ C_{10}^I \leq \max\{Y_2(1/\lambda_m), Y_4(1/\lambda_m)\} - C_{01}^I/\lambda_m \\ \quad \in [a_2, a_4]. \end{cases} \text{for } C_{01}^I$$

Therefore, the corresponding parameters of four curves $Y_i (i = 1, 2, 3, 4)$ can be obtained by fitting the stress–strain curve obtained by Eq. (10), and then, three value ranges of model parameters C_{01}^I and C_{10}^I in Eq. (11) can be determined.

3.1.2 Interval Arrhenius model

The notion of time–temperature equivalent superposition serves as the theoretical basis for high-temperature accelerated testing of rubber, and the conventional Arrhenius model is typically used to describe the nonlinear equivalence between temperature and reaction time scales. In this model, the aging time τ and aging characteristic index P are considered to obey the following functional relationship:

$$P = Ae^{-Kt^{\alpha}}, \tag{12}$$

where P is the performance degradation index of the rubber material at aging time τ, τ is the aging time (days), A is a dimensionless constant, α is the aging reaction time index, $0 < \alpha \leq 1$. K is the aging reaction rate constant related to the thermodynamic temperature, and K obeys the following equation:

$$K = Ze^{-\frac{E_a}{RT}}, \tag{13}$$

where Z is the frequency factor, E is the activation energy of the reaction, R is the ideal gas constant (8.314 J·mol^{-1}·K^{-1}), and T is the temperature in Kelvin.

Taking the logarithm of both sides of Eq. (12) and performing mathematical conversions, we obtain

$$\ln P = -K\tau^{\alpha} + \ln A. \tag{14}$$

We let $y = \mathrm{In}P$, $x = \tau^{\alpha}$, $c = -K$, and $d = \mathrm{In}A$, and Eq. (14) can be written as follows:

$$y = cx + d. \tag{15}$$

Similarly, taking the logarithms of both sides of Eq. (13) and performing a mathematical conversion yield

$$\ln K = -\frac{E_a}{R} \times \frac{1}{T} + \ln Z. \tag{16}$$

We let $y_1 = \mathrm{In}K$, $x_1 = 1/T$, $c_1 = -E_a/R$, and $d_1 = \mathrm{In}K$, and Eq. (16) can be written as follows:

$$y_1 = c_1x_1 + d_1. \tag{17}$$

Eq. (13) can be obtained by analyzing the rubber property degradation curve. If the curve correlation is linear, then $\alpha = 1$. If the relationship is not linear, then $\alpha \in (0, 1)$. At this time, the α value is estimated by approximation criterion, and the criterion for approximation is to make the α value accurate to two decimal places when the I value in Eq. (18) is minimal,

$$I = \sum_{i=1}^{m}\sum_{j=1}^{n}(\bar{p}_{ij} - P_{ij})^2, \tag{18}$$

where $\bar{p}_{ij}$ is the rate of change in the experimental test value of the constant tensile modulus at the jth test point at the ith aging temperature of the rubber, and P_{ij} is the predicted rate of change in the constant tensile modulus at the jth test point at the ith aging temperature.

The interval Arrhenius model proposed in this study introduces the interval radius function $r(t, T)$ and median function $M(t, T)$ based on the traditional model, where Trepresents the test temperature and t represents the test time. As the values of the interval radius and median are obtained by accelerated aging tests, both their equations satisfy the Arrhenius model and can be expressed by Eqs (19) and (20). In practical applications, $M(t, T)$ and $r(t, T)$ are calculated using Eqs (21) and (22), respectively,

$$M(t, T) = A_1e^{-K_1\tau^{\alpha_1}}, \tag{19}$$

$$k(t, T) = A_2e^{-K_2\tau^{\alpha_2}}, \tag{20}$$

$$M(t, T) = \frac{1}{2}(\max(P^I) + \min(P^I)), \tag{21}$$

$$r(t, T) = \frac{1}{2}(\max(P^I) - \min(P^I)). \tag{22}$$

Here A_1, K_1, and α_1 represent the parameters of median fitting curve $M(t, T)$, A_2, K_2, and α_2 represent the parameters

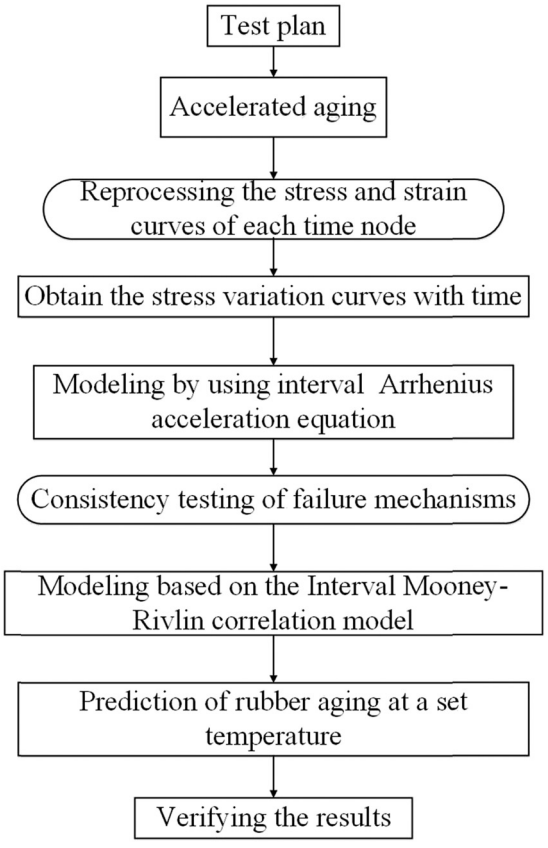

Figure 8: Flow chart of the modeling method for accelerated aging intervals of rubber.

of interval radius fitting curve $r(t, T)$, and P^I represents the accelerated aging test data of rubber; the tensile stress is used in this study.

In interval analysis theory, an interval model problem can be decomposed into two deterministic parameter problem processes. Therefore, the aging property index of rubber can be characterized by the median and interval radii, as shown in Eq. (23).

$$P^I = M(t, T) \pm r(t, T). \tag{23}$$

A consistency check of the failure mechanism is required to verify the availability of the test data. Arrhenius considered the prefactor and activation energy of the reaction to be constants that do not vary with temperature for a given reaction. According to Equation (14), the activation energy obtained by deriving is given by Eq. (24).

$$E_a = -\frac{\mathrm{dIn}K}{\mathrm{d}(1/T)\cdot R}. \tag{24}$$

The reaction activation energy in each temperature interval was calculated using Eq. (24) to confirm the consistency of the failure mechanism of the median and interval radii. Then, $K_i (i = 1, 2)$ satisfying the consistency condition is substituted in Eq. (12) to obtain the interval expression of the material property degradation with respect to time t and temperature T.

3.2 Modeling process

Based on the stress–strain curves obtained from the tensile tests, the curves for the stress fluctuation of the rubber material over time at each strain were fitted. The data on rubber property degradation acquired under various temperatures and strain rates were then used to perform nonlinear fitting of Eq. (12). The interval Arrhenius model and interval M–R model were then used to develop interval acceleration equations for rubber to predict the degradation of aging properties and the rubber lifetime at room

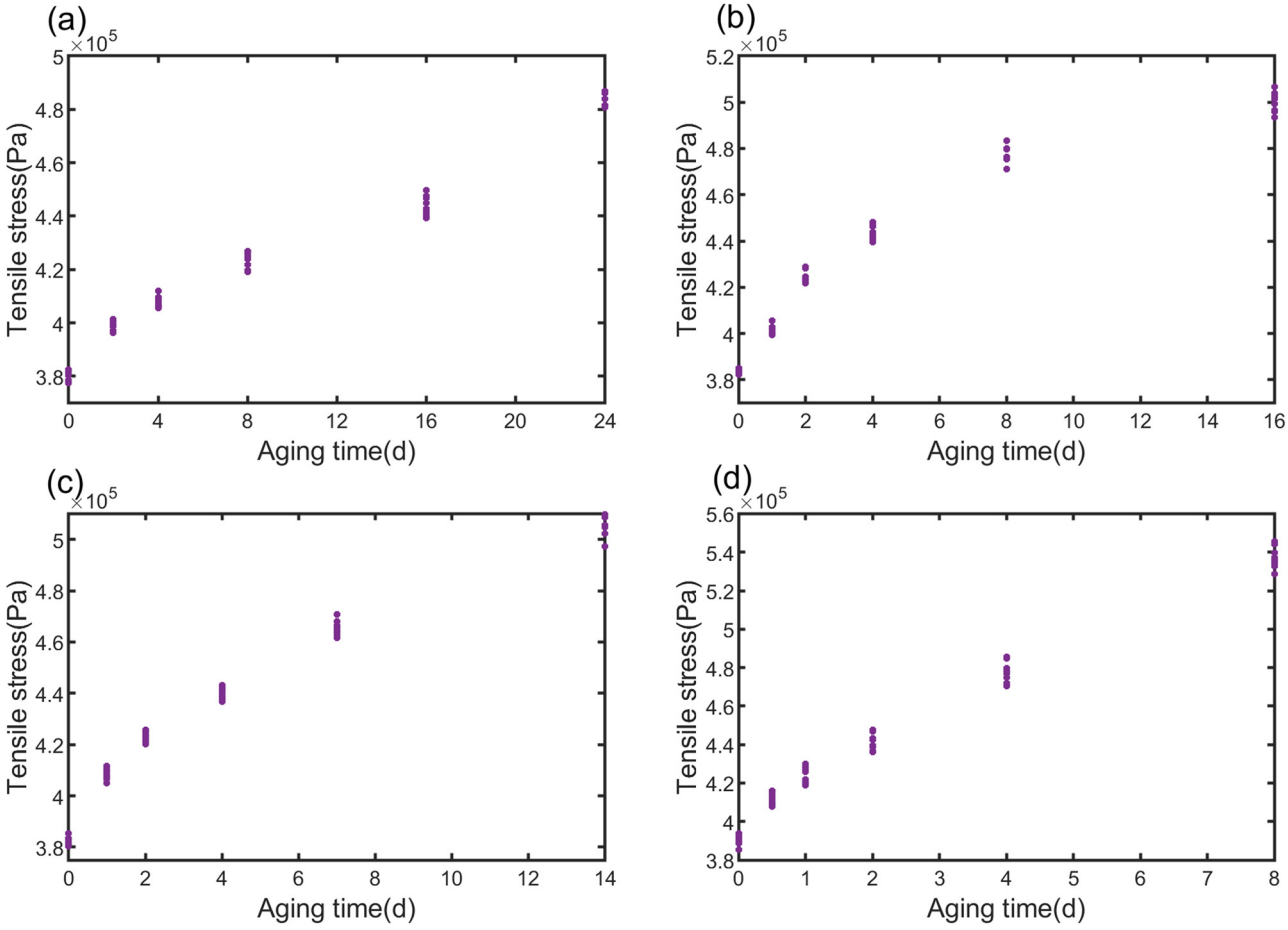

Figure 9: Degradation data of rubber tensile stress with aging time at multiple temperatures: (a) 70, (b) 80, (c) 90, and (d) 100°C.

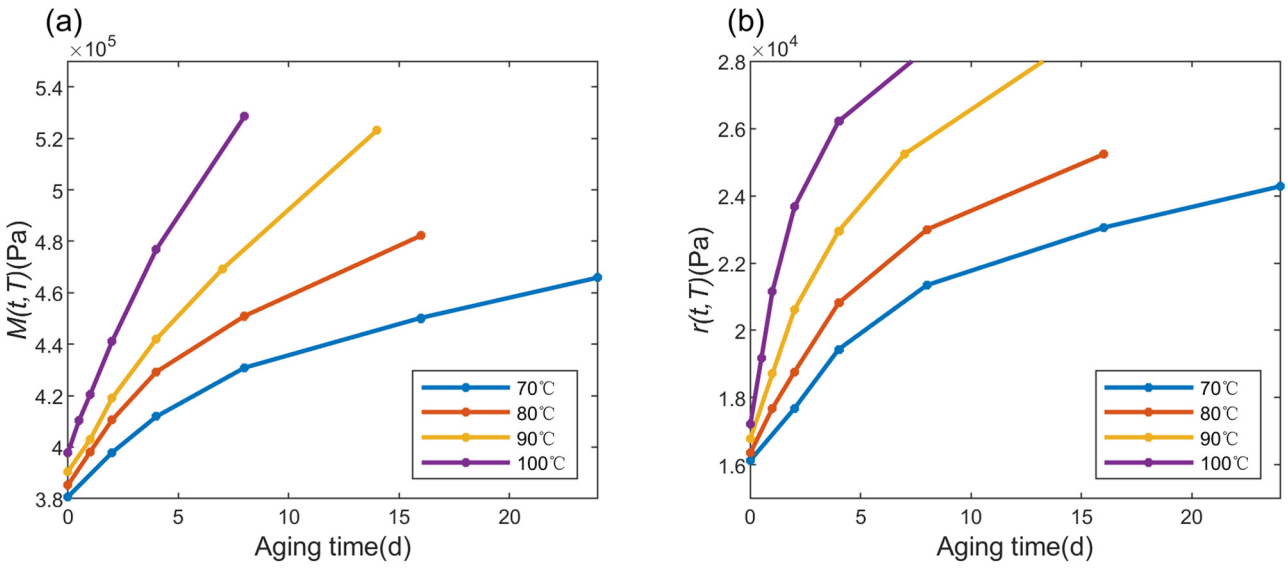

Figure 10: Curves of the rubber performance degradation index at a 10% strain rate: (a) median *M(t, T)* and (b) interval radius *r(t, T)*.

temperature. Figure 8 shows the process flow for the rubber-accelerated aging modeling approach considering the effect of uncertainties.

Taking a 10% strain rate as an example, degradation data of rubber tensile stress with aging time at multiple temperatures were obtained, as shown in Figure 9. Eqs (21) and (22) were used to calculate the median and interval radii, respectively, for different aging times at multiple temperatures. Based on the obtained degradation data of the rubber properties, nonlinear fitting of Eqs (19) and (20) was performed. Fitting parameters $\ln A_i (i = 1, 2)$ and $K_i (i = 1, 2)$ were obtained for the interval Arrhenius model at four temperatures. To confirm the consistency of the failure mechanism of rubber in the accelerated degradation test, the activation energy was calculated using Eq. (24) for different reaction rates ($K_i (i = 1, 2)$) at each temperature interval. The aforementioned technique was then utilized to establish the expressions of stress as a function of aging time and temperature for each strain rate, assuming consistency.

According to the established interval model, the trends of the tensile stress of the rubber material with aging time and aging temperature at different strain rates were obtained. Assuming that the aging time is t days, the stress interval for that aging time at different strain rates can be obtained from Eq. (23) and plotted with $1/\lambda$ as the horizontal coordinate and $\sigma/2(\lambda - \lambda^{-2})$ as the vertical coordinate. Eq. (10) is used to obtain the parameters of the four schematic lines of $Y_i (i = 1, 2, 3, 4)$, and Eq. (11) is applied to determine the ranges for the interval correlation model parameters C_{10}^I and C_{01}^I. It should be noted that the prediction model has the following basic assumptions and limitations: (1) The actual service temperature fluctuation of rubber materials should not be too large. The tensile mechanical properties of rubber at different temperatures will change, and since the model is based on the tensile test data obtained at room temperature (23°C), theoretically it can only predict the properties of rubber materials at room temperature (23°C) after aging at different temperatures. (2) The model takes a 10% strain rate as the interval, and can only calculate the parameter value range of the constitutive model under the strain of rubber material from 10 to 80%, thus the C_{01} and C_{10} parameters obtained from the interval M–R model are only applicable to rubber aging at small and medium strains.

Table 5: Interval model parameters of rubber sample used in this study

Rubber model parameters	All temperatures	70°C	80°C	90°C	100°C	All temperatures
	$\ln A$			K		α
$M(t, T)$	12.8674	0.0258	0.0379	0.0543	0.0762	0.65
$r(t, T)$	9.7013	0.1070	0.1372	0.1732	0.2148	0.44

Table 6: Acceleration coefficient of each aging index at different temperatures

Rubber model aging parameters	$\ln(Z)$	$\frac{E_a}{R}$
$M(t, T)$	9.8102	4618.8867
$r(t, T)$	6.4402	2975.0902

Table 7: Activation energy values as a function of temperature range

	90–100 (°C)	80–90 (°C)	70–80 (°C)
E_{aM}(KJ/mol)	559.3448	555.6568	551.0110
E_{ar}(KJ/mol)	361.7803	359.7995	350.4580

4 Results and discussion

4.1 Parameter identification for the interval Arrhenius model

Figure 10 shows the variation curve of the rubber aging model parameters with aging time at a 10% strain rate.

Table 5 lists the computational results for the rubber interval aging model parameters. Table 6 presents the results of the acceleration model coefficient calculations for each aging index. The computed activation energies are listed in Table 7 for each temperature range.

The activation energy calculations shown in Table 7 confirm the consistency of the rubber failure mechanism in the accelerated aging test, enabling the interval model to be used to forecast the actual aging of the rubber. As described in Section 3.1.2, the interval model can be divided into two parts. Eq. (20) can be used to represent the relationship between the rubber tensile stress and aging time and temperature, while Eqs (25) and (26) show the relationship between the median and interval radii and aging time and temperature, respectively.

$$M(t, T) = e^{12.8674 + e^{9.8102 - 4618.8867/T} \cdot t^{0.65}}, \tag{25}$$

$$r(t, T) = e^{9.7013 + e^{6.4402 - 2975.0902/T} \cdot t^{0.44}}. \tag{26}$$

Using the above method, the expressions for stress as a function of aging time and temperature at each strain rate were established, as listed in Table 8.

4.2 Parameter identification for the interval M–R model

Based on the obtained interval Arrhenius equation, the expressions for the parameters on the left side of Eq. (10) were obtained. The specific parameter values for both sides of Eq. (10) at each strain rate are shown in Table 9 as an example of aging at 60°C for 20 days.

Figure 11 shows the reacquired stress–strain curves with the horizontal coordinates $1/\lambda$ and vertical coordinates $\sigma/2(\lambda - \lambda^{-2})$.

The expressions for the four schematic lines of $Y_i(i = 1, 2, 3, 4)$ were obtained by fitting the above curves using Eq. (10), as shown in Eqs (27)–(30): The parameters of the correlated M–R model obtained from Eq. (11) are shown in Eq. (31).

$$Y_1 = 3.3909 - 0.1794/\lambda, \tag{27}$$

$$Y_2 = 3.8382 - 0.21/\lambda, \tag{28}$$

$$Y_3 = 3.4022 - 0.2109/\lambda, \tag{29}$$

$$Y_4 = 3.7083 - 0.1666/\lambda, \tag{30}$$

Table 8: Interval prediction model for tensile stress of rubber at different strains

Strain (%)	Stress (Pa)
10	$P = e^{12.8674 + e^{9.8102 - 4618.8867/T} \cdot t^{0.65}} \pm e^{9.7013 + e^{6.4402 - 2975.0902/T} \cdot t^{0.44}}$
20	$P = e^{13.2851 + e^{10.3582\,4834.5526/T} \cdot t^{0.54}} \pm e^{10.1992 + e^{8.1224\,3772.6742T} \cdot t^{0.49}}$
30	$P = e^{13.5139 + e^{8.7189\,4154.7351/T} \cdot t^{0.48}} \pm e^{10.5446 + e^{7.1701\,3532.8027/T} \cdot t^{0.49}}$
40	$P = e^{13.7205 + e^{8.623 - 4286.252/T} \cdot t^{0.48}} \pm e^{10.7788 + e^{7.3252 - 3665.4593/T} \cdot t^{0.49}}$
50	$P = e^{13.9156 + e^{8.9013 - 4418.2637/T} \cdot t^{0.54}} \pm e^{10.9681 + e^{7.5563 - 3715.3426/T} \cdot t^{0.48}}$
60	$P = e^{14.1012 + e^{8.9557 - 4513.5041/T} \cdot t^{0.52}} \pm e^{11.1368 + e^{7.5915 - 3625.9913/T} \cdot t^{0.49}}$
70	$P = e^{14.2286 + e^{8.5209 - 4032.5016/T} \cdot t^{0.56}} \pm e^{11.2058 + e^{7.1075 - 3169.1953/T} \cdot t^{0.45}}$
80	$P = e^{14.3542 + e^{8.9512 - 4207.4018/T} \cdot t^{0.49}} \pm e^{11.2696 + e^{7.7975 - 3372.9172/T} \cdot t^{0.52}}$

Table 9: Parameter identification by the M–R model for aged rubber

λ (%)	$1/\lambda$	Mid of $\sigma/2(\lambda-\lambda^{-2})$	Radius of $\sigma/2(\lambda-\lambda^{-2})$
10	10	2.4292	0.1236
20	5	1.9892	0.1001
30	3.3333	1.9429	0.1039
40	2.5	2.012	0.1115
50	2	2.3566	0.1301
60	1.6667	2.9080	0.1679
70	1.4286	4.0154	0.2475
80	1.25	5.9727	0.3886

$$\begin{cases} C_{01}^{I} \in [-0.2109, -0.21], \\ C_{10}^{I} \in [1.2932 - 10 \times C_{01}^{I}, 3.5757 - 1.25 \times C_{01}^{I}] \\ C_{01}^{I} \in [-0.21, -0.1794], C_{10}^{I} \in [3.3909, 3.8382] \\ C_{01}^{I} \in [-0.1794, -0.1666], \\ C_{10}^{I} \in [3.1667 - 1.25 \times C_{01}^{I}, 2.0423 - 10 \times C_{01}^{I}]. \end{cases} \quad (31)$$

4.3 Test verification

Ten samples were obtained for accelerated aging tests at 60 and 25°C to confirm the effectiveness of the proposed interval model. The rubber specimens were held at room temperature (23 ± 2°C) for 24 h before the determination and then subjected to uniaxial tensile testing to obtain the stress–strain curves. After obtaining the stress–strain curves, the parameter $\sigma/2(\lambda - \lambda^{-2})$ values were calculated. The parameter results are shown in Tables 10 and 11, respectively. Tables 12 and 13 present the test results of the parameters of the intrinsic model for different samples calculated using Eq. (3). The degradation of mechanical properties of rubber after aging at 60°C for 20 days and 25°C for 10 days was predicted by the deterministic method

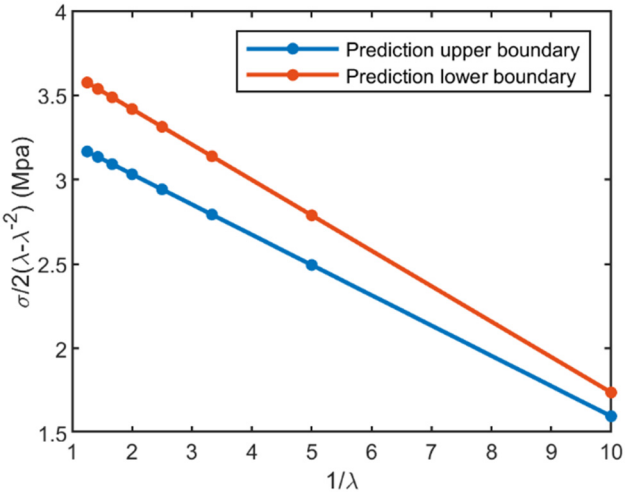

Figure 11: Reacquired interval stress–strain curve of the rubber used in this study.

based on the average value, the interval prediction method without considering the correlation between parameters, and the interval prediction method used in this study. The interval prediction model is shown in Figure 12, which includes measured data from several samples.

As shown in the above figure, the test values of mechanical properties of the tested samples at the set temperature can be accurately covered by the interval prediction model. This indicates that the proposed method for constructing an interval model by introducing interval variables is feasible and effective for predicting the degeneration of mechanical properties of rubber during service. In Figure 12(a), the maximum error between the upper boundary and the measured results is 15%, and the maximum error between the lower boundary and the measured results is 17%. Similarly in Figure 12(b), the maximum error of both boundaries and measurements does not exceed 20%.

Table 10: Values of parameter $\sigma/2(\lambda-\lambda^{-2})$ for each specimen at different strain rates after aging at 60°C for 20 days

Specimens	λ							
	0.1	0.2	0.3	0.4	0.5	0.6	0.7	0.8
1	1.6147	2.5169	3.1079	3.0225	3.4024	3.1525	3.4966	3.2739
2	1.6793	2.7592	3.1216	2.9717	3.307	3.2528	3.4076	3.3998
3	1.6438	2.7433	2.9125	3.2885	3.0966	3.2158	3.469	3.3138
4	1.6352	2.6106	2.8933	3.1661	3.2032	3.367	3.1791	3.1777
5	1.6751	2.5439	3.0992	3.0825	3.2766	3.445	3.2474	3.3714
6	1.6229	2.6208	2.8656	3.1891	3.3913	3.2864	3.4445	3.505
7	1.6932	2.6166	2.8382	3.2363	3.2366	3.4113	3.2219	3.2726
8	1.6052	2.7086	2.9728	3.0662	3.2741	3.2213	3.1484	3.1855
9	1.6022	2.6137	3.1057	3.1994	3.2951	3.3099	3.3109	3.2675
10	1.6378	2.7742	2.932	3.0181	3.3886	3.2461	3.5128	3.437

Table 11: Values of parameter $\sigma/2(\lambda-\lambda^{-2})$ for each specimen at different strain rates after aging at 25°C for 10 days

Specimens	λ							
	0.1	**0.2**	**0.3**	**0.4**	**0.5**	**0.6**	**0.7**	**0.8**
1	1.5483	2.4667	2.829	2.7952	3.0226	3.0107	3.1654	3.1241
2	1.469	2.4892	2.7993	2.9814	3.0904	2.9771	3.2417	3.1903
3	1.4653	2.3846	2.6526	3.0036	2.9755	3.1647	3.0293	3.0335
4	1.5421	2.4162	2.8048	2.99	3.0103	3.0149	3.2315	3.1513
5	1.4984	2.4042	2.6469	2.8147	3.1316	2.9571	3.2425	3.1846
6	1.4549	2.5049	2.8741	2.8853	3.1234	2.9137	3.0433	2.9829
7	1.4648	2.3497	2.8576	2.7622	3.0141	3.2068	2.9704	3.1314
8	1.519	2.5339	2.7542	2.8545	3.124	3.1198	3.1935	3.2668
9	1.507	2.3867	2.7999	2.7979	2.862	3.1768	2.9741	3.0154
10	1.4726	2.4372	2.8827	2.8918	3.0955	3.2016	3.1811	3.1223

However, the maximum errors between the predicted and experimental results of rubber mechanical property parameters based on the average values are 72 and 69%, respectively. The prediction area of the model proposed in this study is reduced by nearly 60% compared to the previous model, and the proposed method can provide a more conservative and accurate life range for the prediction of the life of the rubber material in service, which can avoid the safety problems caused by over-life operation of the rubber products to a certain extent. It can also be seen from Figure 12 that the prediction area of the method is significantly smaller than that of the traditional interval analysis method, which indicates that the correlation between interval parameters affects the prediction accuracy. The interval model used in this study can effectively avoid the influence of errors caused by interval expansion and improve the prediction accuracy.

The research presented above demonstrates the suitability of the recently developed rubber interval model for characterizing the nonlinear stress–strain behavior of rubber-like elastomers at various strain rates. In practice, according to the service temperature and length of service of rubber products, combined with the proposed interval model can calculate the variation range of parameters C_{10} and C_{01}, then based on the failure thresholds in the actual engineering applications, the predicted life intervals of such rubber parts can be obtained.

5 Conclusion

Based on the measured data of accelerated rubber aging, a kinetic equation for the trajectory of accelerated rubber

Table 12: The test results of the parameters of the intrinsic model for different samples after aging at 60°C for 20 days

Intrinsic model parameters	Specimens									
	1	**2**	**3**	**4**	**5**	**6**	**7**	**8**	**9**	**10**
C_{10}	3.5831	3.5738	3.5472	3.6234	3.6152	3.7229	3.6882	3.5825	3.5138	3.5592
C_{01}	−0.1880	−0.1864	−0.1882	−0.1910	−0.1977	−0.2127	−0.2081	−0.1849	−0.1748	−0.1823

Table 13: The test results of the parameters of the intrinsic model for different samples after aging at 25°C for 10 days

Intrinsic model parameters	Specimens									
	1	**2**	**3**	**4**	**5**	**6**	**7**	**8**	**9**	**10**
C_{10}	3.3575	3.4473	3.3593	3.4091	3.391	3.339	3.3696	3.4545	3.2941	3.4596
C_{01}	−0.1802	−0.1965	−0.1901	−0.1881	−0.1931	−0.1814	−0.1913	−0.1939	−0.1778	−0.1984

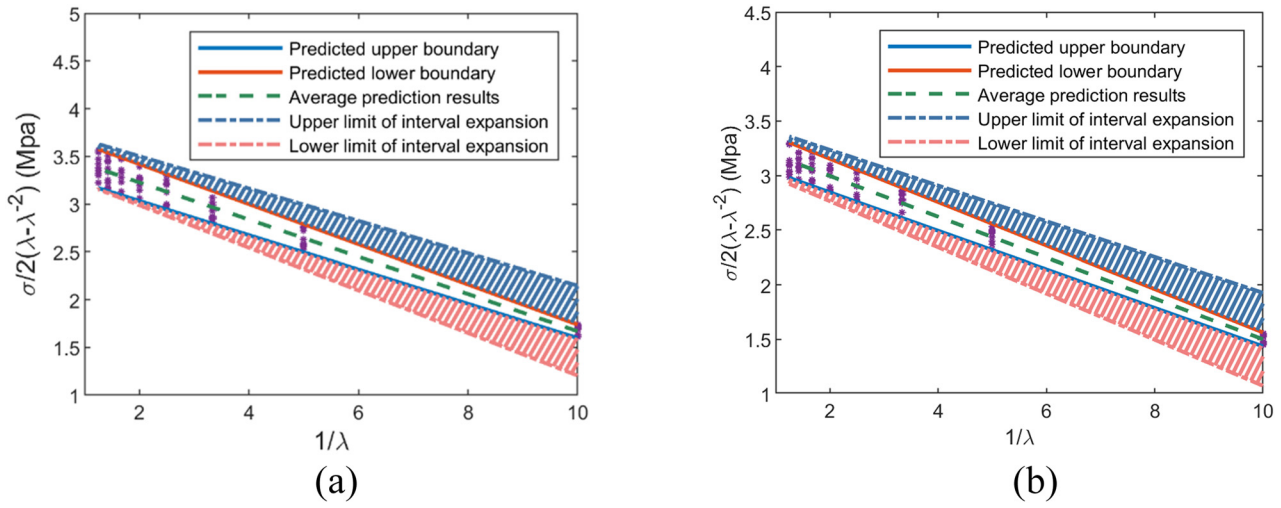

Figure 12: Interval model for the prediction of degradation of rubber mechanical properties: (a) after aging at 60°C for 20 days and (b) after aging at 25°C for 10 days.

aging was established considering the influence of parameter uncertainty and correlation. Based on the conventional Arrhenius model, an interval variable was introduced to represent the uncertainty, and an interval Arrhenius model describing the relationship between tensile stress and temperature under uncertainty was proposed. The interval expansion problem in the linear regression equation was analyzed, the correlation between the parameters of the intrinsic model was verified, and the interval M–R correlation model was used to describe the nonlinear properties of rubber. Experimental evidence was used to confirm the validity of the model. The main findings of this study are as follows:

1) Differences in the mechanical properties of samples of different rubber materials and the effect of uncertainty on the lifetime prediction model must be considered.
2) The prediction results of the proposed model accurately correlate with the measured results with a maximum error of no more than 20%, while the maximum error of the prediction results of the average-based prediction method with the measured data is close to 80%.
3) By considering the correlation between the two interval parameters in the M–R two-parameter model, the constructed prediction model can more accurately characterize the nonlinear mechanical behavior of rubber materials and solves the problem that the range of variation of the interval parameters in the traditional interval M–R model is not consistent with the reality.

The prediction model in this study is based on the tensile test data at room temperature (23°C), and only the effect of temperature on rubber aging is considered. Therefore, the application of the model is premised on meeting the requirement that changes in ambient temperature do not directly affect the properties of rubber materials. It is worth noting that our study only demonstrated the effectiveness of the proposed predictive model in predicting the parameters of the M–R model interval for air spring rubber aging. However, the model developed in this study can be applied to the prediction of other types of rubber products under uncertainty and air aging through feasible extensions, which can provide a new idea for the life prediction of rubber products. Since the interval Arrhenius model developed in this study only includes the prediction of tensile stresses at strains from 10 to 80% (at 10% strain increments), the C_{10} and C_{01} parameters obtained from the interval M–R model are only applicable to rubber aging at small and medium strains.

Further research can consider narrowing the interval envelope based on the interval model to increase the estimation precision, such as adjusting the strain increment. In addition, the influence of additional factors needs to be considered, as rubber products are affected by more than just temperature during service. It is necessary to continue investigating the prediction of rubber performance under combined factors to establish a rubber aging prediction model that is more in line with actual engineering.

Acknowledgments: The authors wish to acknowledge the National Key R&D Program of China for financial support (grant number 2022YFB4300300).

Funding information: This research was funded by National Key R&D Program of China, Grant number 2022YFB4300300.

Author contributions: All authors have accepted responsibility for the entire content of this manuscript and approved its submission.

Conflict of interest: The authors state no conflict of interest.

References

[1] Gent, A. N. *Engineering with rubber: how to design rubber components*, 3rd edn, Carl Hanser Verlag, Munich, 2012.

[2] Gillen, K. T., M. Celina, R. L. Clough, and J. Wise. Extrapolation of accelerated aging data-Arrhenius or erroneous? *Trends in Polymer Science*, Vol. 8, No. 5, 1997, pp. 250–257.

[3] Liu, Q., W. Shi, K. Li, Z. Chen, and H. Liu. Performance degradation prediction and reliability evaluation of rubber aging in natural environment under alternating cyclic thermal load. *IEEE Access*, Vol. 7, 2019, pp. 63027–63035.

[4] Celina, M. C. Review of polymer oxidation and its relationship with materials performance and lifetime prediction. *Polymer Degradation and Stability*, Vol. 98, No. 12, 2013, pp. 2419–2429.

[5] Moghadam, M. K., J. Morshedian, M. Ehsani, M. Bahrami, and H. Saddadi. Lifetime prediction of HV silicone rubber insulators based on mechanical tests after thermal ageing. *IEEE Transactions on Dielectrics and Electrical Insulation*, Vol. 20, No. 3, 2013, pp. 711–716.

[6] Woo, C. S., S. S. Choi, S. B. Lee, and H. S. Kim. Useful lifetime prediction of rubber components using accelerated testing. *IEEE Transactions on Reliability*, Vol. 59, No. 1, 2010, pp. 11–17.

[7] Hartler, G. Parameter estimation for the Arrhenius model. *IEEE Transactions on Reliability*, Vol. 35, No. 4, 1986, pp. 414–418.

[8] Nelson, W. B. *Accelerated testing: statistical models, test plans, and data analysis*, John Wiley & Sons, New York, 2009.

[9] Nelson, W. Analysis of accelerated life test data-Part I: The Arrhenius model and graphical methods. *IEEE Transactions on Dielectrics and Electrical Insulation*, Vol. 4, 1971, pp. 165–181.

[10] Šimon, P., Z. Cibulková, and P. Thomas. Accelerated thermooxidative ageing tests and their extrapolation to lower temperatures. *Journal of Thermal Analysis and Calorimetry*, Vol. 80, No. 2, 2005, pp. 381–385.

[11] Bystritskaya, E. V., A. L. Pomerantsev, and O. Y. Rodionova. Evolutionary design of experiment for accelerated aging tests. *Polymer Testing*, Vol. 19, No. 2, 2000, pp. 221–229.

[12] Le Huy, M. and G. Evrard. Methodologies for lifetime predictions of rubber using Arrhenius and WLF models. *Die Angewandte Makromolekulare Chemie*, Vol. 261, No. 1, 1998, pp. 135–142.

[13] Davies, P. and G. Evrard. Accelerated ageing of polyurethanes for marine applications. *Polymer Degradation and Stability*, Vol. 92, No. 8, 2007, pp. 1455–1464.

[14] Le Saux, V., P. Y. Le Gac, Y. Marco, and S. Calloch. Limits in the validity of Arrhenius predictions for field ageing of a silica filled polychloroprene in a marine environment. *Polymer Degradation and Stability*, Vol. 99, 2014, pp. 254–261.

[15] Gillen, K. T., M. Celina, and R. Bernstein. Review of the ultrasensitive oxygen consumption method for making more reliable extrapolated predictions of polymer lifetimes. *Society of Plastics Engineers. ANTEC,2004: 62nd Annual Technical Conference; 2004 May 16–20; Chicago, IL*, Society of Plastics Engineers, Connecticut, 2004, pp. 2289–2293.

[16] Gillen, K. T., R. Bernstein, and M. Celina. Non-Arrhenius behavior for oxidative degradation of chlorosulfonated polyethylene materials. *Polymer Degradation and Stability*, Vol. 87, No. 2, 2005, pp. 335–346.

[17] Celina, M., K. T. Gillen, and R. A. Assink. Accelerated aging and lifetime prediction: Review of non-Arrhenius behaviour due to two competing processes. *Polymer Degradation and Stability*, Vol. 90, 2005, pp. 395–404.

[18] Wang, Y. S., W. Wang, Q. Liu, Z. B. Cui, and J. Wang. Analysis on the Non-Arrhennius life prediction method of Rubber. *Advanced Materials Research*, Vol. 683, 2013, pp. 366–371.

[19] Liu, Q., W. Shi, Z. Chen, K. Li, H. Liu, and S. Li. Rubber accelerated ageing life prediction by Peck model considering initial hardness influence. *Polymer Testing*, Vol. 80, 2019, id. 106132.

[20] Naveršnik, K. Humidity-corrected Arrhenius equation: The reference condition approach. *International Journal of Phamaceutics*, Vol. 500, No. 1–2, 2016, pp. 360–365.

[21] Mao, S. S. Statistical analysis of accelerated life testing-step-stress models under the exponential distribution case. *Acta Mathematicae Applicatae Sinica*, Vol. 8, No. 3, 1985, pp. 311–316.

[22] Changyong, D., D. Shaojiang, and T. Wei. Modelling for the flow behavior of a new metastable beta titanium alloy by GA-based Arrhenius equation. *Materials Research Express*, Vol. 6, No. 2, 2018, id. 026544.

[23] Zhou, J., J. Yao, H. H. Hu, and Y. Song. Accelerated aging life evaluation method of silicone rubber based on segmented nonlinear Arrhenius model. *Materials Research Innovations*, Vol. 19, No. Sup 5, 2015, pp. 855–860.

[24] Du, R. L., K. Wu, D. A. Xu, C. Y. Chao, L. Zhang, and X. D. Du. A modified Arrhenius equation to predict the reaction rate constant of Anyuan pulverized-coal pyrolysis at different heating rates. *Fuel Processing Technology*, Vol. 148, 2016, pp. 295–301.

[25] Raheem, H. M. and A. M. Al-Mukhtar. Experimental and analytical study of the hyperelastic behavior of the hydrogel under unconfined compression. *Procedia Structural Integrity*, Vol. 25, 2020, pp. 3–7.

[26] Raheem, H. M. and A. M. Al-Mukhtar. Experimental investigation of the effects of infusing a foam into hydrogels on the hyperelastic coefficients. Material design & processing. *Communications*, Vol. 3, No. 4, 2021, id. e180.

[27] Khaniki, H. B., M. H. Ghayesh, R. Chin, and M. Amabili. Hyperelastic structures: A review on the mechanics and biomechanics. *International Journal of Non-Linear Mechanics*, Vol. 148, 2022, id. 104275.

[28] Khaniki, H. B., M. H. Ghayesh, and R. Chin. Theory and experiment for dynamics of hyperelastic plates with modal interactions. *International Journal of Engineering Science*, Vol. 182, 2023, id. 103769.

[29] Khaniki, H. B., M. H. Ghayesh, R. Chin, and L. Q. Chen. Experimental characteristics and coupled nonlinear forced vibrations of axially travelling hyperelastic beams. *Thin-Walled Structures*, Vol. 170, 2022, id. 108526.

[30] Khaniki, H. B., M. H. Ghayesh, R. Chin, and S. Hussain. Nonlinear continuum mechanics of thick hyperelastic sandwich beams using various shear deformable beam theories. *Contin Mech Thermodyn*, Vol. 34, No. 3, 2022, pp. 781–827.

[31] Destrade, M., G. Saccomandi, and I. Sgura. Methodical fitting for mathematical models of rubber-like materials. *Proceedings.*

Mathematical, Physical, and Engineering Sciences, Vol. 473, No. 2198, 2017, id. 20160811.

[32] Marckmann, G. and E. Verron. Comparison of hyperelastic models for rubber-like materials. *Rubber Chemistry and Technology*, Vol. 79, No. 5, 2006, pp. 835–858.

[33] Puglisi, G. and G. Saccomandi. Multi-scale modelling of rubber-like materials and soft tissues: an appraisal. *Proceedings. Mathematical, Physical, and Engineering Sciences*, Vol. 472, No. 2187, 2016, id. 20160060.

[34] Bystritskaya, E. V., A. L. Pomerantsev, and O. Y. Rodionova. Prediction of the aging of polymer materials. *Chemometrics and Intelligent Laboratory Systems*. Vol. 47, No. 2, 1999, pp. 175–178.

[35] Rodionova, O. Y. and A. L. Pomerantsev. Prediction of rubber stability by accelerated aging test modeling. *Journal of Applied Polymer Science*, Vol. 95, No. 5, 2005, pp. 1275–1284.

[36] Lee, S. P. and K. W. Kang. Deformation analysis of rubber seal assembly considering uncertainties in mechanical properties. *Journal of Mechanical Science and Technology*, Vol. 33, No. 7, 2019, pp. 3345–3353.

[37] Liu, L., X. Y. Li, E. Zio, R. Kang, and T. M. Jiang. Model uncertainty in accelerated degradation testing analysis. *IEEE Transactions on Reliability*, Vol. 66, No. 3, 2017, pp. 603–615.

[38] Varga, L., B. Szabó, I. G. Zsély, Zempléni A., and Turányi T. Numerical investigation of the uncertainty of Arrhenius parameters. *Journal of Mathematical Chemistry*, Vol. 49, No. 8, 2011, id. 1798.

[39] Woo, C. S., W. D. Kim, and J. D. Kwon. A study on the material properties and fatigue life prediction of natural rubber component. *Materials Science and Engineering: A Structure Materials*, Vol. 483, 2008, pp. 376–381.

[40] Shao, Y., and R. Kang. A life prediction method for O-ring static seal structure based on physics of failure. *2014 Prognostics and System Health Management Conference (PHM-2014 Hunan), 2014 Aug 24–27, Zhangjiajie, China*, IEEE, 2014, pp. 16–21.

[41] Korba, A. G., A. Kumar, and M. Barkey. A hyper-elastic thermal aging constitutive model for rubber-like materials. *Journal of Elastomers and Plastics*, Vol. 52, No. 8, 2020, pp. 677–700.

[42] Nagy, T. and T. Turanyi. Uncertainty of Arrhenius parameters. *International Journal of Chemical Kinetics*, Vol. 43, No. 7, 2011, pp. 359–378.

[43] Héberger, K., S. Kemény, and T. Vidóczy. On the errors of Arrhenius parameters and estimated rate constant values. *International Journal of Chemical Kinetics*, Vol. 19, No. 3, 1987, pp. 171–181.